Ecological Modelling 491 (2024) 110669

Contents lists available at ScienceDirect

Ecological Modelling

journal homepage: www.elsevier.com/locate/ecolmodel

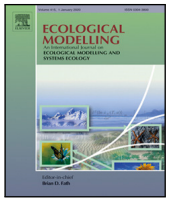

A Bayesian approach to projecting forest dynamics and related uncertainty: An application to continuous cover forests

Mari Myllymäki [a,*], Mikko Kuronen [a], Simone Bianchi [a], Arne Pommerening [b], Lauri Mehtätalo [c]

[a] Natural Resources Institute Finland (Luke), Latokartanonkaari 9, FI-00790 Helsinki, Finland
[b] Department of Forest Ecology and Management, Faculty of Forest Sciences, Swedish University of Agricultural Sciences SLU, Skogsmarksgränd 17, SE-90183 Umeå, Sweden
[c] Natural Resources Institute Finland (Luke), Yliopistokatu 6B, FI-80100 Joensuu, Finland

ARTICLE INFO

Keywords:
Bayesian statistics
Continuous cover forestry
Forest growth
Global credible interval
Individual-based model
Random effects

ABSTRACT

Continuous cover forestry (CCF) is forest management based on ecological principles and this management type is currently re-visited in many countries. CCF woodlands are known for their structural diversity in terms of tree size and species and forest planning in CCF needs to make room for multiple forest development pathways as opposed to only one management target. As forest management diversifies and management types such as CCF become more common, models used for projecting forest development need to have a generic and flexible bottom-up design. They also need to be able to handle uncertainty to a larger extent and more comprehensively than is necessary with single, traditional forest management types. In this study, a spatial tree model was designed for analyzing a data set involving 18 plots from CCF stands in Southern Finland. The tree model has specific ingrowth, growth and mortality model components, each including a spatially explicit competition effect involving neighboring trees. Approximations were presented that allow inference of the model components operating in annual steps based on time-series measurements from several years. We employed Bayesian methodology and posterior predictive distributions to simulate forest development for short- and long-term projections. The Bayesian approach allowed us to incorporate uncertainties related to model parameters in the projections, and we analyzed these uncertainties based on three scenarios: (1) known plot and tree level random effects, (2) known plot level random effects but unknown tree level random effects, and (3) unknown random effects. Our simulations revealed that uncertainties related to plot effects can be rather high, particularly when accumulated across many years whilst the length of the simulation step only had a minor effect. As the plot and tree effects are not known when tree models are applied in practice, in such cases, it may be possible to significantly improve model projections for a single plot by taking one-off individual-tree growth measurements from the plot and using them for calibrating the model. Random plot effects as used in our tree model are also a way of describing environmental conditions in CCF stands where other traditional descriptors based on stand height and stand age fail to be suitable any more.

1. Introduction

Continuous cover forestry (CCF) is a type of forest management which is based on ecological principles (e.g., Kruse et al., 2023). Definitions of CCF usually include a number of tenets that can vary between countries and organizations involved (Pommerening and Murphy, 2004; O'Hara, 2014; Pommerening, 2023). The most prominent tenet of CCF is the requirement to abandon the practice of large-scale clearfelling and to favor more environmentally friendly harvesting and natural regeneration methods. There are also many semi-synonyms to CCF that we adopted in this paper; while objectives, definitions and standards implied by these semi-synonyms can differ (Palik et al., 2021; Puettmann et al., 2015; Kruse et al., 2023), our modeling approach also applies to any other semi-synonym.

In Fennoscandia, rotation forest management (RFM) has been the dominant forest management type for more than 50 years. RFM typically involves homogeneous even-aged, mono-species forest stands, simple forest structure with mostly one canopy layer and final harvesting through clearfelling where all trees are removed from site in a single operation and the forest stand is eventually replanted.

The historic roots of CCF can be traced back to at least the second half of the 19th century (Peng, 2000; Pommerening and Murphy, 2004). In recent decades, CCF was re-discovered in different parts of

* Corresponding author.
E-mail address: mari.myllymaki@luke.fi (M. Myllymäki).

https://doi.org/10.1016/j.ecolmodel.2024.110669
Received 25 September 2023; Received in revised form 20 December 2023; Accepted 23 February 2024
Available online 1 March 2024

the world (Kruse et al., 2023). At the same time there has also been an increasing dissatisfaction of European societies with industrialized forms of plantation and RFM. CCF is now being promoted in Fennoscandia due to societary pressure and the potential for better economic profitability on poor sites and for its possible benefits to biodiversity, carbon sequestration and storage, and to the landscape (see, e.g., Kuuluvainen et al., 2012; Lundqvist, 2017; Hertog et al., 2022). Also, forest management types in which no explicit choice is made between RFM and CCF are fostered in Fennoscandia (Pukkala, 2018).

As the forest structure resulting from different forest management types becomes more complex, there is a need for more generalized modeling approaches that can handle any forestry situation and spatial tree structure. In Central Europe, this change to more generalized model designs started in the early 1990s and included individual-oriented, spatially explicit bottom-up approaches that allowed the greatest possible flexibility in terms of tree size and species composition but also in terms of spatial forest structure (Pretzsch, 2009). The most flexible tree models for projecting forest dynamics are spatially explicit, since such models are able to project any type of horizontal and vertical forest structure. Spatially explicit tree models typically include spatial interactions between trees by accounting for the local neighborhood of each tree (e.g., Garcia, 2014; Nothdurft, 2020). The modeling of thinnings and other interventions typical of CCF are also made markedly easier in spatial tree models. Thus, spatially explicit approaches are particularly attractive in the context of CCF and other management types where much structural variability may occur within stands, and, as a benefit, model projections can also include traditional RFM as a special case. In uneven-aged CCF forests, the appearance of tree seedlings and saplings as a consequence of natural regeneration is mostly heterogeneous, and the modeling of these small trees plays a crucial role, especially when forest development is projected for a long time period (Lappi and Pukkala, 2020).

The predictors of spatially explicit tree models typically include tree size, a measure of environmental conditions (in forestry also referred to as 'site quality') and a characteristic of tree interaction which is usually termed competition index (Reineke, 1933; Biging and Dobbertin, 1995).

Competition indices are often used to describe how the interaction among trees including the competition for resources decreases growth compared to the maximum growth possible at a given site. They can be interpreted as proxies describing the resource allocation in individual trees. Spatial (or distance-dependent) competition measures take the location of each tree into account. A large number of different competition measures are documented in the literature (e.g., Schneider et al., 2006; Eerikäinen et al., 2007; Häbel et al., 2019; Bianchi et al., 2020; Zhou et al., 2022). Some of these are defined only at the locations of subject trees, while others can quantify competition loads at any location in a forest stand. Particularly in forest ecology, spatially explicit tree modeling have much focused on describing spatial tree interactions by so-called competition kernels, which are kernels of probability density functions describing how trees affect the growth and/or survival of its neighboring trees (Pommerening and Grabarnik, 2019). In this context, the term individual based models (IBMs) or growth-interaction models is often used (Cronie et al., 2013; Redenbach and Särkkä, 2013; Häbel et al., 2019). As previously mentioned, the emergence of new trees is often heterogeneous in CCF; thus, in our study, we considered the effect of neighboring trees not only on growth and mortality, but also on ingrowth, by means of a spatially explicit individual-tree competition measure defined at any location in the stand. Such general competition measures are likely to contribute to flexibility as required in models applied in the context of CCF.

Environmental conditions, such as climate and soil, determine the growth potential of the trees of a forest stand. They can be described by characteristics related to the ground vegetation (Cajander, 1949) or alternatively by certain stand height and basal-area characteristics (Pretzsch, 2009; Lappi and Bailey, 1988; Salas-Eljatib, 2020). However, many assumptions used in tree models developed for RFM do not hold in the context of CCF (see the extensive review from Skovsgaard and Vanclay, 2008). Particularly, stand age is not defined in CCF, i.e., the trees of a forest stand can potentially have a considerable age range and the age of individual trees is commonly unknown.

From a statistical point of view, different types of uncertainties are present in projections carried out by any tree model. Such uncertainties are likely to increase when tree models are generalized so that they can include CCF scenarios. Bayesian methodologies have been applied, e.g., in the context of tree growth (Nothdurft, 2020), tree mortality (Wyckoff and Clark, 2000), plant interactions (Schneider et al., 2006), and forecasting forest yield at stand level (Nyström and Ståhl, 2001), but we are not aware of many tree models that explicitly include uncertainty in the modeling process and projections (Green and Strawderman, 1996; Wilson et al., 2019). The Bayesian statistical approach for parameter estimation provides a natural way to include the parameter uncertainty in tree model projections (Gelman et al., 2014; Sirkiä et al., 2015).

The parameters of any tree model typically need to be estimated from empirical data, such as from long-term forest monitoring sites. Such time series data have a nested structure (e.g., repeated measurements within trees, several trees within plots and several tree measurements within calendar years). The nested structure of the data implies complex dependence structures between observations that should be taken into account in parameter estimation and inference. A natural way to consider this dependence is through multilevel models including group effects, which are often commonly known as random effects (Bürkner, 2017; Mehtätalo and Lappi, 2020). Random effects can also be predicted for the groups represented by the observed data, which allows predictions at different levels of hierarchy in the data. However, when applying the model for the projection of forest stands that were not part of the data used for fitting the model, the random effects are not known. If the variability between the forest monitoring plots is large, the unknown random effect may then potentially be a large source of errors in growth predictions.

When predictions are carried out for long time periods, the predictive model is applied iteratively, e.g., in annual or multi-year steps according to the model framework. After the first step, the growth model therefore uses predictors (e.g., tree size, competition index) based on predictions made in the previous simulation step. In classic, frequentistic statistical models, the predicted values are estimates of a conditional expectation of the variable, which have a lower variance than the true values. Furthermore, if the explanatory variables enter the model after a nonlinear transformation, they can introduce a bias to the predictions (see also Wilson et al., 2019). These problems can be avoided by using predictive distributions instead of the classic prediction. One possibility is to apply Monte Carlo simulations (e.g., Kangas, 1999). In this study, we employed Bayesian inference where predictions naturally are generated from the posterior predictive distribution, i.e., the distribution of unobserved values conditional on the observed values (e.g., Gelman et al., 2014).

The aim of this study is

(i) to introduce and analyze a spatially explicit tree model that is suitable for CCF, and not restricted to a specific forest management type,
(ii) to handle uncertainties of model projections in a realistic way,
(iii) to allow predictions for any time intervals, not only for those that were specific to the tree survey periods of the monitoring sites which provided the data for the model fitting
(iv) to include all necessary components for the projection of forest development, but still keep the model sufficiently simple to be widely applicable.

We hypothesized that the proposed tree model - equipped with Bayesian inference - is sufficiently flexible to simulate CCF forest development along with the associated uncertainty. We modeled ingrowth, growth

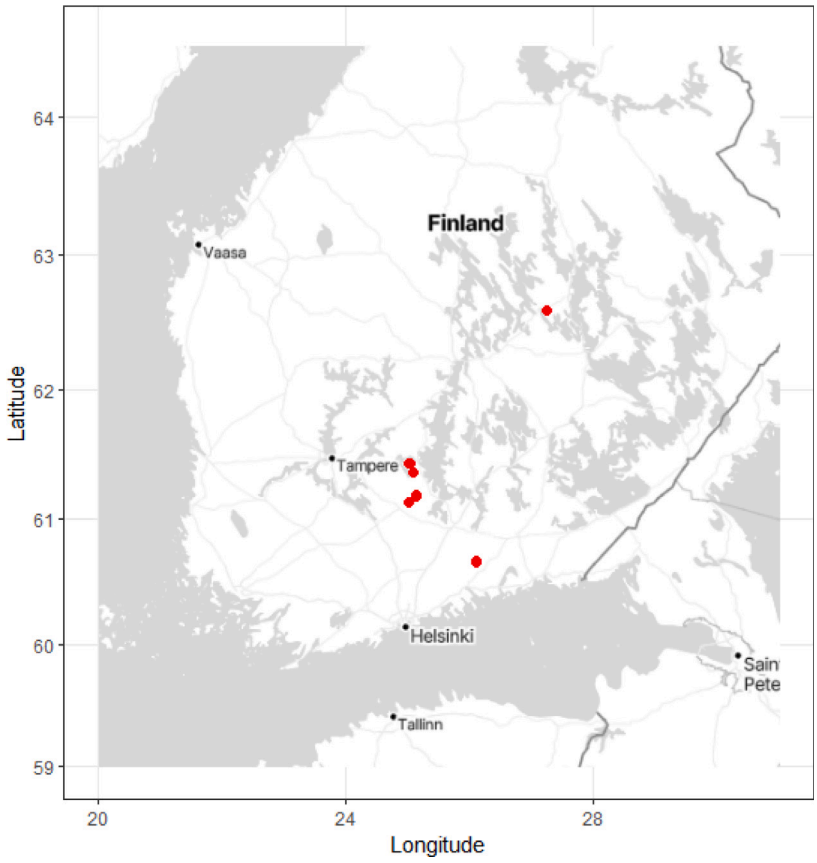

Fig. 1. The locations of the ERIKA plots in Southern Finland. Background map (C) National Land Survey of Finland 2022.

and mortality of trees, and as part of our validation, projected the forest plots involved for a period of 15 years without thinning events. We quantified the influence of different lengths of projection steps on the accuracy of the model output. We further studied how the knowledge of random plot and tree effects influence the accuracy of the predictions: in addition to the 15-year projections that did not include thinnings, we also studied the accuracy associated with a projection over 100 years. The latter involved thinnings that were based on simple rules and followed official recommendations. Finally, we discussed potential model applications and extensions.

2. Material and methods

2.1. Data

We analyzed data from 18 Norway spruce (*Picea abies* (L.) Karst.) dominated stands in five areas (2–7 stands in each) in Southern Finland (Fig. 1). The data belong to a long-term experiment of permanent CCF sample plots involving selective harvesting, conducted in the ERIKA research project at the Natural Resources Institute Finland (Valkonen et al., 2020b). The stands were naturally regenerated and had a history of complex structures and partial harvests. Utilizing the existing structural complexity, selective thinning was carried out in all the stands between 1985 and 1988. The selective thinning was repeated in 16 stands in 1996. Four stands were not thinned in 1996 due to low total basal area. Selective thinning was repeated again in all stands in 2011. As part of the thinning operations, all trees with defects or damage were removed first, and then healthy trees mainly from larger diameter classes (>25 cm) were cut until a certain target basal area was achieved. Since thinning and harvesting operations tend to be both selective and very similar in CCF, we used both terms as synonyms in this study. Sixteen stands belonged to the submesic *Myrtillus* type site classification, suggesting medium fertility, while four stands can be described as mesic *Oxalis-Myrtillus* woodland communities, suggesting higher fertility (Cajander, 1949; Tonteri et al., 1990). Using environmental characteristics, namely temperature sum (the accumulated temperature over 5 °C in degree days), site classification, and an index determined by the proximity to the sea and lakes, the site index was estimated as the expected height of the dominant trees in an even-aged, monospecies stand of Norway spruce at the age of 100 years in the same place (Hynynen et al., 2002). Here we settled on an approach where the site quality classes based on ground vegetation were transformed to values that describe the site index for even-aged management. In our data analyses, the index describes the environmental conditions of the stand, although not with the same meaning as for even-aged RFM stands.

We had data available from single plots of size 40 m × 40 m that were set up in the central part of each stand. Stand size ranged from 1.5 ha to 2.0 ha and the plots were chosen to represent the site and structural variation within each stand. Tree measurements in the plots commenced in 1991 and were repeated every fifth growing season until 2016; only in two cases, a plot was measured after six growing seasons, and in one case after four growing seasons. For each tree, species, stem diameter at breast height (dbh), tree height, and local stem-center coordinates were recorded. The thinnings in 1996 and 2011 were carried out immediately after the measurements. The site index of the 20 plots varied between 25.9 m and 33 m and mean dbh between 5.8 and 15 cm (Table 1). There was much variation across plots and trees concerning the amount of competition that was exerted by neighboring trees at the location of a tree and measured by the competition index (Table 1). Additional details on the experimental design, study sites and measurements can be found in Bianchi et al. (2020), Hynynen et al. (2019) and Valkonen et al. (2020b).

Table 1
Summary of the (a) plot-specific site index, mean stem diameter (dbh) and mean relascope basal area (RBA) competition index (minimum, mean, maximum), and (b) tree dbh and RBA competition index (10% quantile, mean and 90% quantile). The tree-specific RBA is defined in Eq. (1) (Section 2.2.1); mean RBA of a plot is the mean over all trees of the plot.

(a) Plot level	Min	Mean	Max
Site index	25.9	28.4	33
Mean dbh [cm]	5.8	9.5	15
Mean RBA [m^2/ha]	10	15	21
(b) Tree level	**10%**	**Mean**	**90%**
dbh [cm]	0.6	9.0	24
RBA [m^2/ha]	6	15	26

In total, the data available to modeling included 17153 growth observations (change in stem diameter between two consecutive measurements) from 5206 trees, with an absolute mean annual stem diameter growth rate of 2 mm and an interquartile range of 0.7 to 2.9 mm. For modeling tree mortality, we had 18 423 observations of tree status live or dead, originating from 5635 trees in total. Among these observations there were 1206 trees that had died, mostly as a consequence of wind and snow, followed by competition and harvesting damage (Valkonen et al., 2020a). Further, a total of 3360 trees reaching or surpassing a height of 1.3 m above ground level (referred to as ingrowth trees) were observed, on average 40 ingrowth trees per measurement time and sample plot or 49 ingrowth trees per hectare and year. According to the management plan (dated 1996 and 2011), a total of 1732 trees were cut in the 18 plots altogether and less than 400 trees were harvested or were missing for other reasons. These trees were excluded from the modeling data immediately after the thinning events.

Norway spruce (*Picea abies*) amounted to 75% of the total basal area across all plot measurements. The proportions of Scots pine (*Pinus sylvestris* L.), European aspen (*Populus tremula* L.), and birch (*Betula pendula* Roth and *Betula pubescens* Ehrh.) were all between 4%–8%. Among the ingrowth trees, 57% were Norway spruce. The proportions of aspen and birch were 4%–7%, but 25% of the ingrowth trees were other broadleaves. We modeled all species together, because the numbers of trees of species other than Norway spruce were rather low.

2.2. Tree model

Our tree model for predicting stand dynamics includes three components: ingrowth, stem diameter and height growth, and mortality. All three components of forest development are influenced by tree competition. The competition is modelled in a spatially explicit way (Section 2.2.1). The model components are independent and do not share any parameters. All three models operate in annual steps. We did not model harvests.

2.2.1. Competition

In this study, we used a competition index that is based on the concepts of basal area of larger trees (BAL; Wykoff, 1990) and that of relascope sampling simulated at the location of each tree i (Eerikäinen et al., 2014) with a basal area factor (BAF) $q = 2$. This implies that all trees with a basal area larger than that of subject tree i contributed to the competition index of tree i, provided they were included in a simulated relascope sample carried out at the location of tree i with a BAF of $q = 2$. Formally, the relascope basal area (RBA) index for tree i at plot p at time t is

$$H_{pi,t} = q \sum_{j \neq i} 1\left(\frac{d_{pj,t}}{\mathrm{dist}_{i,j}} > 2 \cdot \sqrt{q}, d_{pj,t} > d_{pi,t}\right), \quad (1)$$

where $\mathrm{dist}_{i,j}$ is the distance between the locations of the trees i and j of plot p and $d_{pi,t}$ is the stem diameter of tree i in plot p at time t.

The RBA index can be interpreted as the sum of influences of neighboring trees that are larger than the subject tree i: Each tree j is assumed to have a zone of influence that extends up to a distance $d_{pj,t}/(2 \cdot \sqrt{q})$ from its location. The competition load of tree i is equal to the sum of influences of those (larger) trees whose zone of influence overlaps the location of tree i.

The individual influences of all trees in plot p can also be summed up at any location x in plot p to yield the competition field

$$H_{px,t} = q \sum_{j} 1\left(\frac{d_{pj,t}}{\mathrm{dist}_{x,j}} > 2 \cdot \sqrt{q}\right), \quad (2)$$

where $\mathrm{dist}_{x,j}$ is the distance between location x and tree j in plot p. The value of the competition field is equal to the competition index (Eq. (1)) computed for a tree of size 0 at location x and corresponds to the basal area per hectare sampled at location x using relascope sampling and a BAF of q.

We used the RBA index (Eq. (1)) in the growth and mortality model components, and the competition field (Eq. (2) in the ingrowth submodel. While growth and mortality are specific to each existing tree, the ingrowth model component takes care of the emergence of new trees at any location x in plot p.

2.2.2. Ingrowth

We assume that new trees emerge in a time interval ranging from time t to $t+1$, according to a Poisson process with intensity

$$\lambda_{p,t}(x) = \exp\left(\alpha_0 + u_p^{\text{ingrowth}} + \alpha_1 \frac{H_{px,t}}{10} + \alpha_2(\mathrm{SI}_p - 28) + \alpha_3 \frac{\mathrm{GDD5}_{pt}}{1000}\right), \quad (3)$$

where α_0, α_1, α_2 and α_3 are model parameters, $u_p^{\text{ingrowth}} \sim N(0, \sigma^2_{u,\text{ingrowth}})$ is the random plot effect, $H_{px,t}$ is the value of competition field (Eq. (2)) at location x at time t, SI_p is the site index of plot p, and $\mathrm{GDD5}_{pt}$ is the temperature sum for plot p in year t (see Mbogga et al., 2009). The constants in Eq. (3) were used to coarsely standardize the covariates.

2.2.3. Growth

Our stem diameter growth model has the following conceptual form:

$$\begin{aligned}\text{future stem diameter} = {} & \text{current stem diameter} + \\ & \text{potential growth} \times \text{competition effect} + \\ & \text{error}\end{aligned} \quad (4)$$

According to this concept, potential growth can be understood as growth that could be observed if the tree grew in the open landscape in absence of any competition from other trees, and this potential growth is reduced by inter-tree competition (see e.g., Pommerening et al., 2011; Cronie et al., 2013; Häbel et al., 2019). Our tree height sub-model has the same conceptual form. More precisely, our stem diameter and tree height sub-models for tree i in plot p for the next year $t+1$ are

$$d_{pi,t+1} = d_{pi,t} + f^{\mathrm{d}}_{\mathrm{pot}}(d_{pi,t}) \cdot H^{\text{d-trans}}_{pi,t} + \epsilon^{\mathrm{d}}_{pi,t+1}, \quad \text{and} \quad (5)$$

$$h_{pi,t+1} = h_{pi,t} + f^{\mathrm{h}}_{\mathrm{pot}}(h_{pi,t}) \cdot H^{\text{h-trans}}_{pi,t} + \epsilon^{\mathrm{h}}_{pi,t+1}, \quad (6)$$

respectively, where

$$f^{\mathrm{d}}_{\mathrm{pot}}(d) = d^{\beta^{\mathrm{d}}_1} \exp\left(\beta^{\mathrm{d}}_0 + u_p^{\text{d-growth}} + v_{pi}^{\text{d-growth}} + \beta^{\mathrm{d}}_2 \frac{d-10}{10} + \beta^{\mathrm{d}}_3(\mathrm{SI}_p - 28) + \beta^{\mathrm{d}}_4 \mathrm{thinning}_t + \beta^{\mathrm{d}}_5 \frac{\mathrm{GDD5}_{pt}}{1000}\right) \quad (7)$$

and

$$f^{\mathrm{h}}_{\mathrm{pot}}(h) = h^{\beta^{\mathrm{h}}_1} \exp\left(\beta^{\mathrm{h}}_0 + u_p^{\text{h-growth}} + v_{pi}^{\text{h-growth}} + \beta^{\mathrm{h}}_2 \frac{h-10}{10} + \beta^{\mathrm{h}}_3(\mathrm{SI}_p - 28) + \beta^{\mathrm{h}}_4 \mathrm{thinning}_t + \beta^{\mathrm{h}}_5 \frac{\mathrm{GDD5}_{pt}}{1000}\right). \quad (8)$$

Here $\beta^{\mathrm{d}}_0, \ldots, \beta^{\mathrm{d}}_5$ and $\beta^{\mathrm{h}}_0, \ldots, \beta^{\mathrm{h}}_5$ are fixed effect parameters, $u_p^{\text{d-growth}}$ and $u_p^{\text{h-growth}h}$ are random plot effects, $v_{pi}^{\text{d-growth}}$ and $v_{pi}^{\text{h-growth}}$ are random tree effects, and $\epsilon^{\mathrm{d}}_{pi,t+1}$ and $\epsilon^{\mathrm{h}}_{pi,t+1}$ are the residuals. The variable $\mathrm{thinning}_t$ accounts for the frequently observed fact that trees are unable to use

newly available growing space immediately after thinning (Mehtätalo et al., 2014) and indicates whether more or less than 5 years elapsed since the last thinning. It is $\text{thinning}_t = 1$ for the years $t = 1996, \dots, 2000$ and $t = 2011, \dots, 2015$, and 0 otherwise. Further, the competition effects are equal to

$$H_{pi,t}^{\text{d-trans}} = 1 - \exp\left(-10\nu^{\text{d}}/H_{pi,t}\right), \quad \text{and} \tag{9}$$

$$H_{pi,t}^{\text{h-trans}} = 1 - \exp\left(-10\nu^{\text{h}}/H_{pi,t}\right), \tag{10}$$

where ν^{d} and ν^{h} are additional model parameters and $H_{pi,t}$ is the competition index (Eq. (1)). This transformed competition effect scales the competition index value to the scale $[0, 1]$; the transformation was chosen following Häbel et al. (2019). The smaller ν^{d}, the smaller $H_{pi,t}^{\text{trans}}$ and the larger the effect of competition on the growth of tree i. Similar to the ingrowth model (Eq. (3)), the constants in Eqs. (7) and (9) are used for coarse standardization of the covariates. The random plot effects $(u_p^{\text{d-growth}}, u_p^{\text{h-growth}})$ and random tree effects $(v_p^{\text{d-growth}}, v_p^{\text{h-growth}})$ are assumed to follow the zero-mean two-dimensional normal distributions with variances $(\sigma^2_{u,\text{d-growth}}, \sigma^2_{u,\text{h-growth}})$ and $(\sigma^2_{v,\text{d-growth}}, \sigma^2_{v,\text{h-growth}})$, and correlations ρ_u and ρ_v, respectively. The residuals of the two model components, $(\epsilon^{\text{d}}_{pi,t+1}, \epsilon^{\text{h}}_{pi,t+1})$, are also assumed to follow the two-dimensional normal distribution with variances $\sigma^2_{\epsilon\text{-d}}$ and $\sigma^2_{\epsilon\text{-h}}$, and correlation ρ_ϵ.

2.2.4. Mortality

We modeled mortality using a generalized linear model with Bernoulli response and the complementary log–log link function. We hypothesized that large trees mainly died as a consequence of diseases and windthrow, while small trees predominantly died because of competition. Therefore, we assumed that the probability of a tree i in plot p to die in a time interval from t to $t+1$ depends both on the current size of the tree and influence of the other trees. Our final mortality model also includes a quadratic form of the competition index and, thus, its linear predictor is defined as

$$\pi_{pi,t} = \gamma_0 + \gamma_1 \frac{d_{pi,t} - 10}{10} + \gamma_2 \frac{H_{pi,t}}{10} + \gamma_3 \frac{H^2_{pi,t}}{100} + u_p^{\text{mortality}} + \gamma_4(\text{SI}_p - 28), \tag{11}$$

where γ_0, γ_1, γ_3 are model parameters, $u_p^{\text{mortality}} \sim N(0, \sigma^2_{u,\text{mortality}})$ is the random plot effect, and the constants result from the coarse standardization for estimation and interpretation purposes. The probability of tree i to die is then $1 - \exp(-\exp(\pi_{pi,t}))$.

2.3. Inference

The recorded data provided tree observations at survey times $t_1, t_2, \dots, t_n$, for example, in our study for every fifth year with some exceptions of four- and six-year intervals. Therefore, for the inference of our model operating in annual steps, we needed some simplifying assumptions and resulting approximations (see Section 2.3.1). Employing these approximations, we performed Bayesian inference (Section 2.3.2) and model evaluation using posterior predictive check with multiple characteristics (Section 2.3.3). Finally, we simulated forest dynamics according to different scenarios, both for a 15-year period without thinnings (Section 2.3.4) and for 100 years, this time applying thinnings as described in Section 2.3.5.

2.3.1. Approximations for the inference

We assumed that the observation intervals are short compared to the tree growth rate so that the effects of the neighboring trees as modeled by the competition index (Eq. (1)), field (Eq. (2)) and the temperature sum (GDD5) are approximately constant over the five-year observation periods. Therefore, the nonlinear predictors $\mu^{\text{d}}_{pi,t} = f^{\text{d}}_{\text{pot}}(d_{pi,t}) \cdot H^{\text{d-trans}}_{pi,t}$ and $\mu^{\text{h}}_{pi,t} = f^{\text{h}}_{\text{pot}}(h_{pi,t}) \cdot H^{\text{h-trans}}_{pi,t}$ of the growth model are approximately constant on the interval ranging from t to $t+s$. This implies that the mean absolute annual growth of stem diameter during s years is

$$\frac{d_{pi,t+s} - d_{pi,t}}{s} \approx \mu^{\text{d}}_{pi,t} + \frac{1}{s}\sum_{t}^{t+s} \epsilon^{\text{d}}_{pi,t+1} \overset{d}{=} \mu^{\text{d}}_{pi,t} + \epsilon^{\text{d}}_{pi,t,s},$$

where $\epsilon^{\text{d}}_{pi,t,s} \sim N(0, (\frac{1}{\sqrt{s}}\sigma^2_{\epsilon\text{-h}})^2)$, and $\sigma^2_{\epsilon\text{-h}}$ is the residual error in the growth sub-model (Eq. (5)), and an analogous term applied to tree height growth. Here $X \overset{d}{=} Y$ denotes that X and Y have the same distribution.

In the ingrowth model, we approximated the competition field $H_{px,t}$ (Eq. (2)) of plot p by a piecewise constant function evaluated at the center points of a 1 m × 1 m grid, in a similar manner as, e.g., in Rue et al. (2009), Møller et al. (1998) and Kuronen et al. (2021). Based on our assumption, the intensity (Eq. (3)) according to which the ingrowth trees emerge stays approximately the same over the observation period. Then, according to the ingrowth sub-model, the number n of ingrowth trees on a grid cell of size 1 m × 1 m during an observation period of s years is Poisson distributed with intensity $s\lambda_{p,t}(x)$. This means that a standard generalized linear model applies with offset $\log s$.

Based on our assumption, the linear predictor $\pi_{pi,t}$ of the mortality model (Eq. (11)) is also approximately the same over an observation period of s years. Given the model parameters, the probability of tree i in plot p to die in a time interval ranging from t to $t+s$ is therefore $1 - \exp(-\exp(\log s + \pi_{pi,t}))$. The complementary log–log link function conveniently allows to specify the model as a standard generalized linear model with offset $\log s$.

2.3.2. Parameter estimation

The models introduced in Section 2.2 were fit using the R package brms (Bürkner, 2017). The brms package is specialized in fitting Bayesian generalized (non)linear multivariate multilevel models using 'Stan' (Stan Development Team, 2022) for full Bayesian inference. We obtained 4000 samples from the posterior distribution of the parameters of each model, with effective sample sizes of model parameters between 400 and 5000.

Bayesian inference requires specifying prior distributions to all parameters of the models. In our study, we applied uninformative priors for all parameters (Gelman et al., 2014). The ingrowth and mortality models used the default flat prior distributions of the brms package for all parameters. For the growth model we specified other priors for some of the parameters: The prior of $\sigma^2_{\epsilon\text{-d}}$ and $\sigma^2_{\epsilon\text{-h}}$ was exponential with a mean of 1000, for ν-parameters (Eqs. (9) and (10)) the prior was exponential with a mean of 10, and for $f^{\text{d}}_{\text{pot}}(d_{pi,t})$ and $f^{\text{h}}_{\text{pot}}(h_{pi,t})$, a normal distribution with a standard deviation of 1000 was used.

2.3.3. Model evaluation

We applied posterior predictive check (Gelman et al., 2014) with different characteristics to evaluate the goodness-of-fit of our forest dynamics model as follows: To compare model predictions with observed data for as long a period as possible, we chose to consider the longest period not involving any thinnings, namely 1996–2011. As starting population we used the tree patterns in 1996, excluding the trees that were harvested in 1996 and a few trees that went missing by 2001. With each set of parameter values of the 4000 posterior samples (see Section 2.3.2), we then simulated forest development for each plot across the 15-year period including ingrowth, growth and mortality. At their emergence, the ingrowth trees were assigned stem diameters of 0.1 cm and heights of 1.35 m. As a result we obtained 4000 realizations from the posterior predictive distribution of our tree model. We then calculated different characteristics for each simulation, resulting in posterior predictive distributions of these characteristics (a)–(h) explained in the following.

Our plot-level characteristics of main interest were

(a) the total basal area of trees and
(b) the total volume of trees

in 2001, 2006 and 2011. The tree volume was obtained by the variable form-factor volume equation proposed by Kangas et al. (2023) which requires stem diameter and height as input variables. Further, we compared the observed and simulated tree patterns of 2011 by the

(c) numbers of trees in different stem diameter classes ([5, 10), [10, 15), [15, 20), [20, 25), … , [60, 65) cm),
(d) pair correlation functions $g(r)$,
(e) mark variograms $\gamma_m(r)$ of tree stem diameters, and
(f) mean height of trees in different stem diameter classes ([5, 10), [10, 15), [15, 20), [20, 25), [25, 30), ≥30 cm).

These characteristics (c)–(f) were computed for trees with stem diameters ≥5 cm. We evaluated the smallest trees through

(g) the numbers of ingrowth events in the periods 1996–2001, 2001–2006 and 2006–2011, and

the mortality through

(h) the volume (m^3/ha) of the trees that died in the same three periods.

Characteristics (d) and (e) summarize the spatial patterns of observed and simulated trees including their stem diameters as so-called marks (e.g., Illian et al., 2008). The pair correlation function $g(r)$ describes the spatial structure of the tree pattern relative to the pattern of complete spatial randomness (CSR, Poisson forest): values $g(r) > 1$ indicate more and values $g(r) < 1$ indicate less points at distance r apart from each other than would be expected under CSR. By contrast, the mark variogram $\gamma_m(r)$ measures dependencies in the stem diameter marks of two trees that are distance r apart from each other: if $\gamma_m(r) < 1$, then the difference between the stem diameters of trees with distance r apart from each other tends to be smaller than the average difference, while $\gamma_m(r) > 1$ suggests larger difference. The reference case $\gamma_m(r) = 1$ corresponds to independent stem diameters of trees.

We summarized the posterior predictive distributions of the characteristics (a)–(h) using global envelopes (Myllymäki et al., 2017; Myllymäki and Mrkvička, 2023). The presented 95% global envelopes represent the central regions in which 95% of the posterior predictive simulations of the characteristic lies; the remaining 5% of the simulations are outside the region for some year t, stem diameter class, distance r or period, depending on the characteristic.

2.3.4. Scenarios

For the aforementioned 15-year simulation, we considered three different scenarios corresponding to increasing levels of uncertainties, namely

(i) a simulation where both plot and tree effects were known,
(ii) a simulation where only the plot effects were known, and
(iii) a simulation where both plot and tree effects were unknown.

In our modeling work, we estimated all random effects. Case (i) compares the full model with the data. However, the plot and tree effects are not known when tree models are applied in practice (case (iii)). If measurements of tree growth are available for some trees of the plot, the random plot effects can be predicted, e.g., by applying mixed-effect model calibration (Mehtätalo and Lappi, 2020) or a Bayesian approach (Sirkiä et al., 2015). Case (ii) gives information on the maximum benefit that can be obtained by using such an approach. In all simulations, the random effects were drawn from their posterior distributions. In the case of an unknown random effect of plot p or tree i, each posterior sample was drawn from the posterior distribution of a randomly chosen existing plot or tree, allowing a different plot or tree to be chosen each time. Hereby the posterior draws represent the variation across existing plots or trees.

We calculated the 15-year simulations using both annual and five-year time steps in separate model simulations to understand the potential problems caused by simulation intervals that are shorter than five years. In simulation practice, the need for annual simulation steps can arise, for example, when a growth model is used for updating forest data to match a current point in time or when thinning operations are scheduled for a time within a 5-year simulation period. Annual simulation steps are also useful for harmonizing data sets collected in different years; such updated data are often required in forest planning and in large national and international research projects. Annual values of competition effects and temperature sum (GDD5) were applied in annual steps, while the five-year step simulations were based on the competition quantified in the first year and on the average GDD5 of the five-year period.

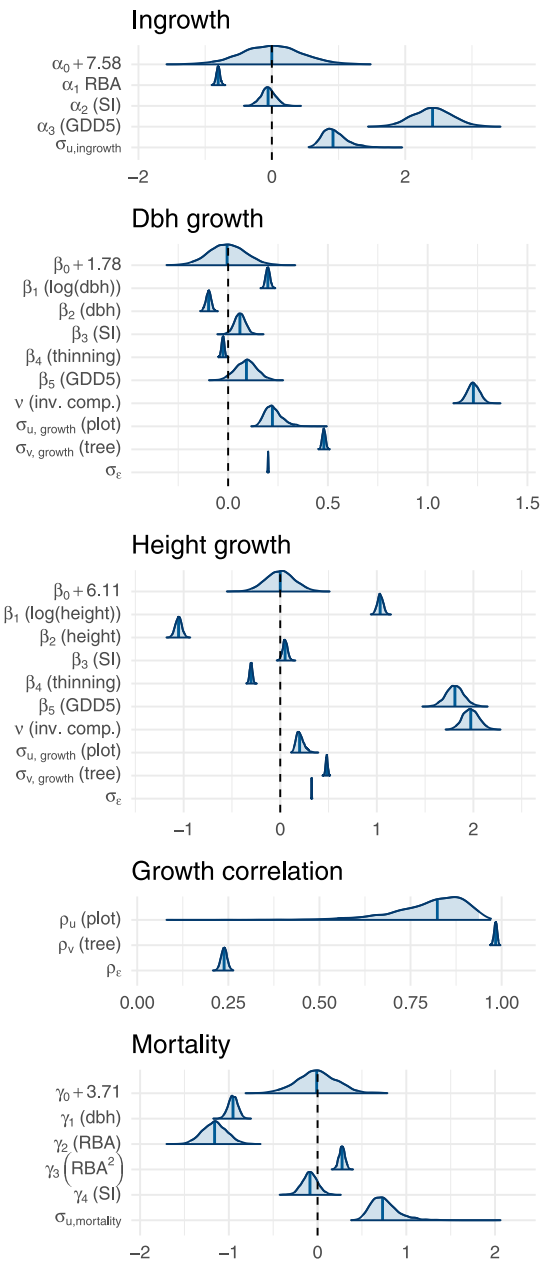

Fig. 2. Posterior distributions of the parameters of the ingrowth sub-model (Eq. (3)), stem diameter (dbh) and height growth sub-model (Eqs. (5)–(6)) and mortality model component (Eq. (11)). The solid vertical lines in the densities denote the posterior means. The names in brackets after the parameters refer to the respective variables.

2.3.5. Long-term projection including thinnings

To study the projections and the corresponding prediction intervals over a long time period, we also simulated forest development

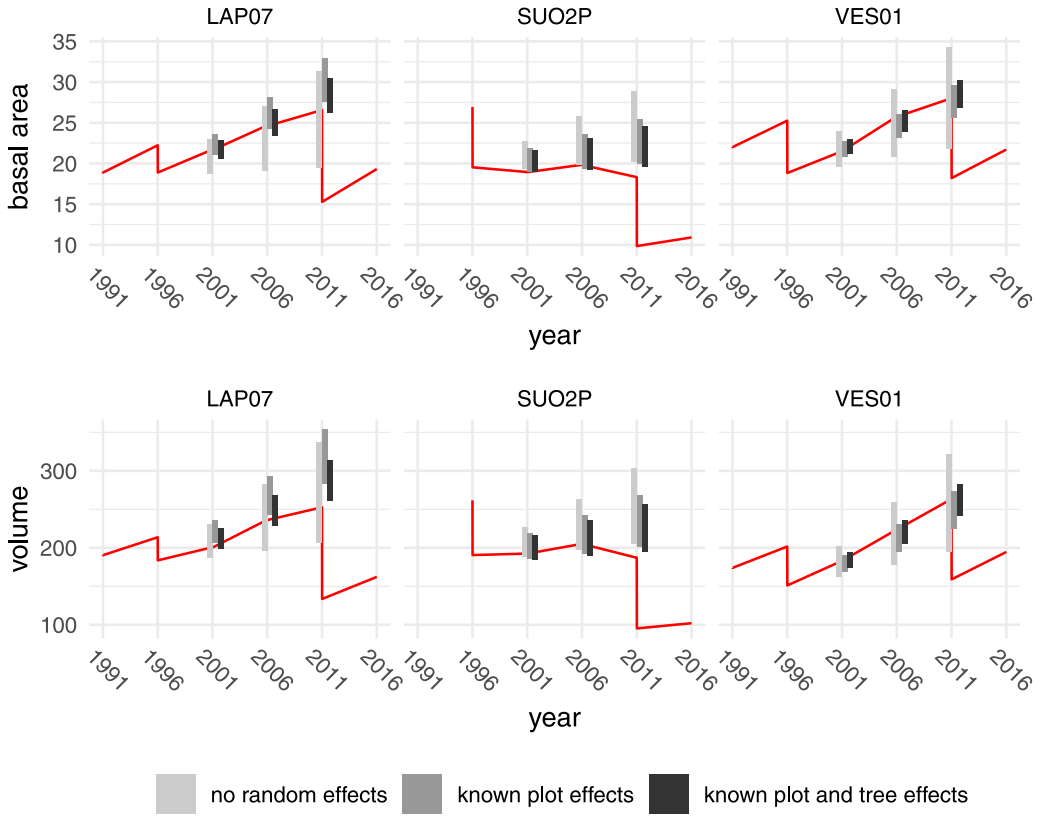

Fig. 3. Total basal area (m^2/ha) and total volume (m^3/ha) in 2001, 2006 and 2011 for three plots VES01, LAP07, SUO2P and three different scenarios (gray bars, see legend). The solid lines represent the observed values. The area covered by each of the three different gray bars corresponds to the 95% global envelopes computed from the posterior predictive distribution based on 5-year time steps.

for 100 years, based on the 1996 patterns as the starting population. In these simulations, we mimicked the thinnings applied in the plots (Bianchi et al., 2020) as follows. We aimed at a residual basal area of 12 m^2 ha^{-1} according to the forest management recommendations in open heathland forests in southern Finland (Tapio, 2023). Thinnings were applied every five years, if the basal area exceeded 22 m^2 ha^{-1}, which is the limit that the basal area should exceed before thinning is recommended. For simplification, we removed trees in random order until the residual basal area of 12 m^2 ha^{-1} was achieved. In these simulations, we monitored the total yield of volume, i.e., the sum of the current volume of live trees and the volume removed across the years from 1996 to the current year. The temperature sum (GDD5) was obviously not known for this period: the GDD5 values observed for 1996–2023 were used, and fixed to the average of the last five years (2019–2023) in the following simulation years.

3. Results

3.1. Parameter estimates

The site index did not affect ingrowth or mortality but had a mild effect on growth: the posterior distributions of the corresponding coefficients in the ingrowth (Eq. (3)) and mortality sub-model (Eq. (11)) were around zero, while the coefficient of the site index in the stem diameter and height growth sub-models (Eqs. (5) and (6)) were slightly positive (Fig. 2). The temperature sum (GDD5) has a positive effect both on ingrowth and growth. The influence of neighboring trees as described by the RBA-index (Eqs. (1) and (2)) decreased ingrowth. This influence also decreased growth, as assumed by the growth sub-model (Eqs. (5)–(6)). For mortality, the effect of RBA was such that a moderate amount of competition led to a lower mortality probability. It should be noted that large trees by definition (Eq. (1)) cannot have a high competition load. Furthermore, in the mortality model, stem diameter had a negative effect, i.e., small trees were more likely to die which matches field observations (Monserud and Sterba, 1999). In the growth sub-model, the coefficient associated with the thinning indicator variable was negative, suggesting that growth was slower up to five years after a thinning, as expected. The random plot and tree effects related to stem diameter and height growth were highly correlated.

The variability between trees was higher than that between plots. The variation between plots was also high compared to the effect of the site index (posterior median (50% uncertainty interval)): the standard deviation of the stem diameter related plot effects is 3.6 (2.8–5.2) times the coefficient of the site index. Therefore, a symmetric 95% uncertainty interval of the plot effects corresponds to a 14-m (11–20 m) variability in the site index.

3.2. 15-Year simulations

In this section, plot VES01 represents the example of a plot where the predictions were rather good with respect to all chosen characteristics. SUO2P is an example where unexplained factors affected the forest development. Further, LAP07 is an example in the Lapinjärvi region, where the forest development was also potentially affected by factors not included in our models. The simulation results of all 18 plots are presented in the Supplementary Materials.

The observed basal area and volume values mostly lie between the 95% global envelopes of posterior predictive distributions, particularly for scenarios (i) and (iii) (Figs. 3, S1 and S2). For scenario (ii), where tree effects were unknown, the observed data were outside the 95% global envelopes of the predictions in a few more cases, e.g., plot LAP07. Further, the results for plots SUO2P and EVO02 (see Supplementary Materials) show an unexpected drop in basal area in 2006.

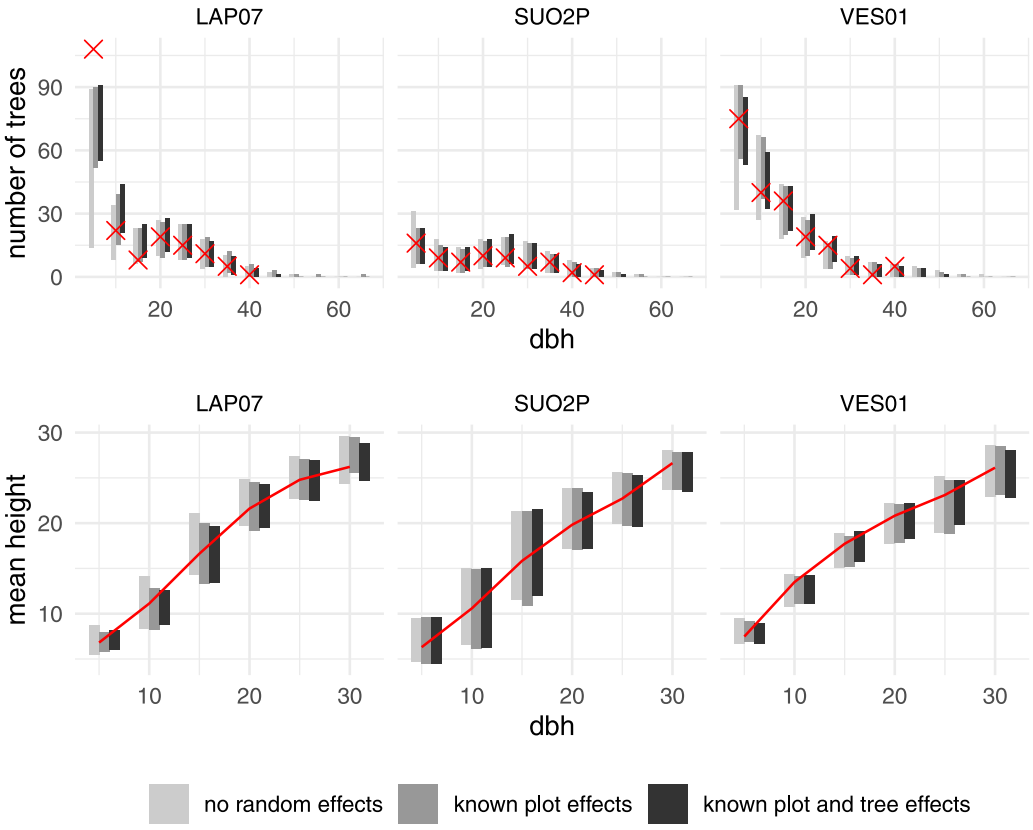

Fig. 4. Total number of trees and the mean height in different stem diameter (dbh) classes in 2011 for three plots VES01, LAP07, SUO2P and three different scenarios (gray bars, see legend). The solid line and red crosses represent the observed values. The area covered by each of the three different gray bars corresponds to the 95% global envelopes computed from the posterior predictive distribution based on 5-year time steps.

Here unexplained factors have affected the growth, as discussed in Section 4. With known random effects, the variability of the posterior predictive distributions of basal area is rather low, and considerably higher when the random effects are unknown. In general, the uncertainty increases a bit with unknown random tree effects, but much more with unknown random plot effects.

Regarding the stem diameter distributions (Fig. 4 and S3), the variations in the numbers of trees with stem diameters ≥5 cm appear to be captured rather well. In plot LAP07, only the number of trees in the smallest stem diameter class is larger than predicted by the model. The simulated height distributions were similar to the observed distributions (Figure S4), and the mean heights in different stem diameter classes (Fig. 4 and S5) were realistic compared to the height–diameter curves estimated using the same data (Siipilehto et al., 2023). The spatial characteristics of the simulated patterns of trees were also similar to the corresponding observed characteristics (Fig. 5), except for plot EVO02 (Figures S6 and S7).

The numbers of ingrowth trees and the basal area of the dead trees were simulated rather adequately (Figs. 6, S8 and S9). When both the plot and tree effects were unknown (scenario (iii)), the numbers of ingrowth trees had very large variability. The number of ingrowth trees varies highly across the plots, making this number a rather difficult variable to be predicted. Judging by the spatial characteristics (Figure S10), the dispersion of these smallest trees was not completely adequately projected by our model. The observed patterns of ingrowth trees are more clustered in some plots than our model predicts. Some extraordinary events (such as storms, bark beetles) led to rather high observed mortality in some plots, but this is still within the model variability.

3.3. Comparison of simulations with annual and 5-year steps

In the previous section, we presented the results of simulations progressing in 5-year steps (between 1996 and 2011), i.e., largely following the temporal pattern of re-measurements in the monitoring plots with only few exceptions. As explained in Section 2.3.4, there are situations where the simulation in one-year steps is helpful.

When comparing the results obtained from using 1- and 5-year simulation steps, we detected some small differences in the posterior predictive distributions for the total basal areas (Figs. 7 and S11–S13) and stem diameter distributions (Figs. 8 and S14–S16): The variability of the basal area predictions was a bit larger when 1-year steps were applied. Regarding the stem diameter distributions, there were also some small differences, but with no clear trend. The model did not show any major problems in projections based on annual time steps. It appears that the use of short simulation steps is largely fine.

3.4. Comparison of the effects of the site index and plot effect

To study the effect of the site index and plot effect, we considered plot VES01. We computed the posterior mean basal area after 15 years assuming that the site index would be either 25.9 m (minimum of the data), 28.4 m (mean of the data) or 33 m (maximum of the data) and that the plot effect in the growth model would be either zero or $\pm 1.96\hat{\sigma}_{u,\text{d-growth}}$ cm, where $\hat{\sigma}_{u,\text{d-growth}} = 0.228$ cm is the posterior mean of the standard deviation of the plot effect. The plot effects in the height growth, ingrowth and mortality sub-models and the tree effects in the diameter and height growth model components were simulated according to the unknown plot and tree effects scenario.

Basal area after 15 years of simulation varied from 25 to 31 m^2/ha along with the site index (zero plot effect), whereas the plot effect led to variation ranging from 23 to 32 m^2/ha (Table 2). Thus, the plot had a somewhat larger effect on the mean basal area than the site index.

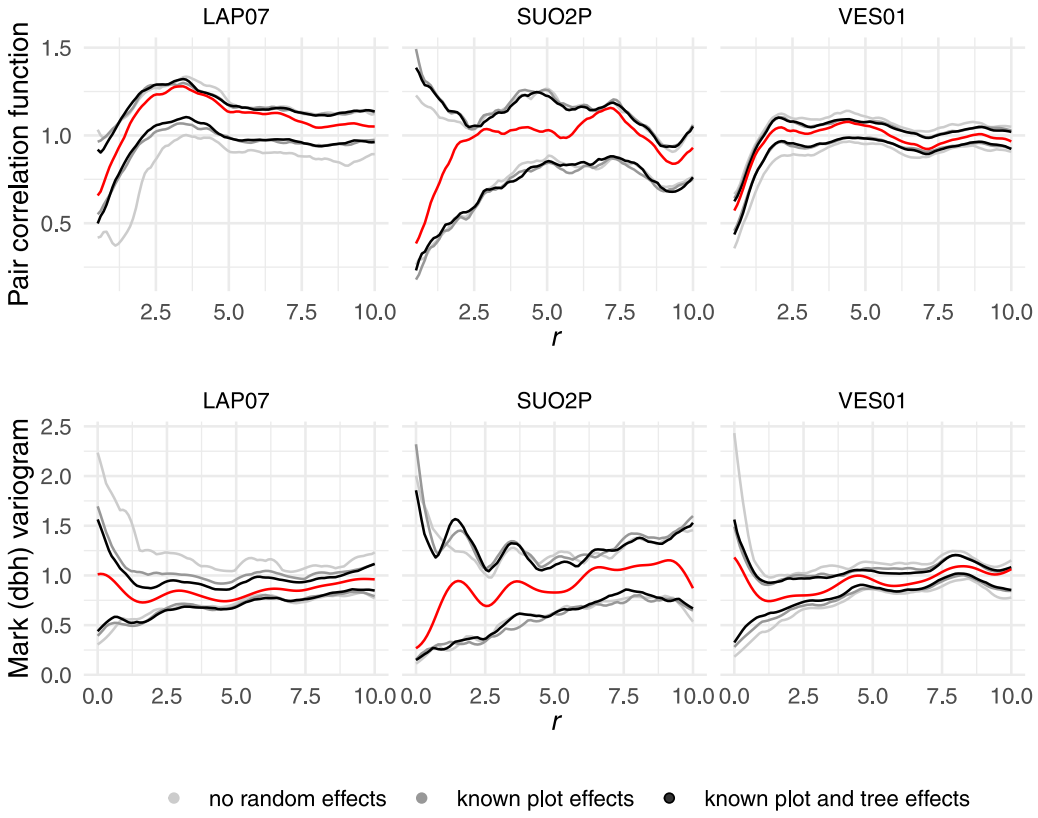

Fig. 5. The pair correlation function $g(r)$ and the mark variogram $\gamma_m(r)$ of stem diameter (dbh), computed for the trees with dbh ≥ 5 cm in the three plots VES01, LAP07, SUO2P in 2011. Red curves correspond to the observed characteristics, gray curves represent the three different scenarios given in the legend. The band between two curves of each scenario corresponds to the 95% global envelope from the posterior predictive distribution based on 5-year time steps.

Table 2
Posterior mean basal area (and 95% uncertainty interval) in plot VES01 after 15 years assuming minimum, maximum and mean site index (SI) of the plots and either no plot effect or a plot effect of magnitude $\pm 1.96\hat{\sigma}_{u,\text{growth}}$.

SI/Plot effect	$-1.96\hat{\sigma}_{u,\text{growth}}$	0	$1.96\hat{\sigma}_{u,\text{growth}}$
Minimum		25.1 (20.4, 28.3)	
Mean	23.5 (19.8, 25.9)	26.8 (22.7, 29.5)	32.3 (27.7, 36)
Maximum		30.5 (25.5, 35.5)	

3.5. Long-term simulation

Finally, we simulated the forest development for 100 years using 5-year steps including thinnings carried out to achieve the recommended residual basal area of 12 m^2/ha^{-1} every time when the current stand basal area exceeded 22 m^2/ha^{-1}, as explained in Section 2.3.4. The amount of uncertainty in the total yield of basal area (Figure S17) and volume (Figs. 9 and S18) given known random effects was moderate. It should be noted that the simulations were carried out under the assumption that the environmental conditions would not change after the first 28 years in the 100 years of the long-term simulation. With unknown random effects, the yield, however, turned out to be highly uncertain. For example, the total volume yield over 100 years in plot LAP07 ranged from 500 to 1800 m^3/ha when the random effects were not known and from 1300 to 1900 m^3/ha when the plot effects were known. The same can be concluded for the total yield of basal area (Figure S21).

4. Discussion

CCF is increasingly considered an alternative in Finland and other European countries where until recently RFM was the standard. The tenets of CCF, as documented in the international literature (Pommerening and Murphy, 2004; O'Hara, 2014; Franklin et al., 2018), suggest a greater diversity of forest structure and a wider range of forest development pathways than what is currently known for traditional RFM. In addition, climate change is likely to add even more variability to the development of forest ecosystems. This situation requires tree models that are both as general as possible and sufficiently detailed to simulate the influence and evolution of forest structure including the associated uncertainties.

In our study, we introduced a spatial tree model to meet these requirements. The Bayesian methods were used for estimating the corresponding model parameters and their distributions. Following this, we simulated CCF forest development from the posterior predictive distribution of the tree model according to three different scenarios. In this process, we explicitly took parameter uncertainties into account. We simulated stand dynamics based on ingrowth, growth, and mortality model components, each including the effect of neighboring trees. Random tree and plot effects were incorporated in the models according to the structure of the observed data. The contribution of the tree and plot effects to the predictive performance was also analyzed.

Our model captured the forest development of the observed CCF data set adequately, as indicated by various characteristics that we used for evaluating the behavior of the tree model. As with any model approach, there is naturally room for improvement. Particularly, the observed ingrowth of regeneration trees in the plots has a high variability that was not completely reproduced by our current tree model. The ingrowth model component could, for example, be extended by a cluster point process model (see e.g., Kuronen et al., 2021), but according to our previous experience, such an approach is computationally rather demanding and might still not capture all the variability present in the spatial structure of the smallest trees. Site quality information within plots might also help to explain the spatial patterns of ingrowth

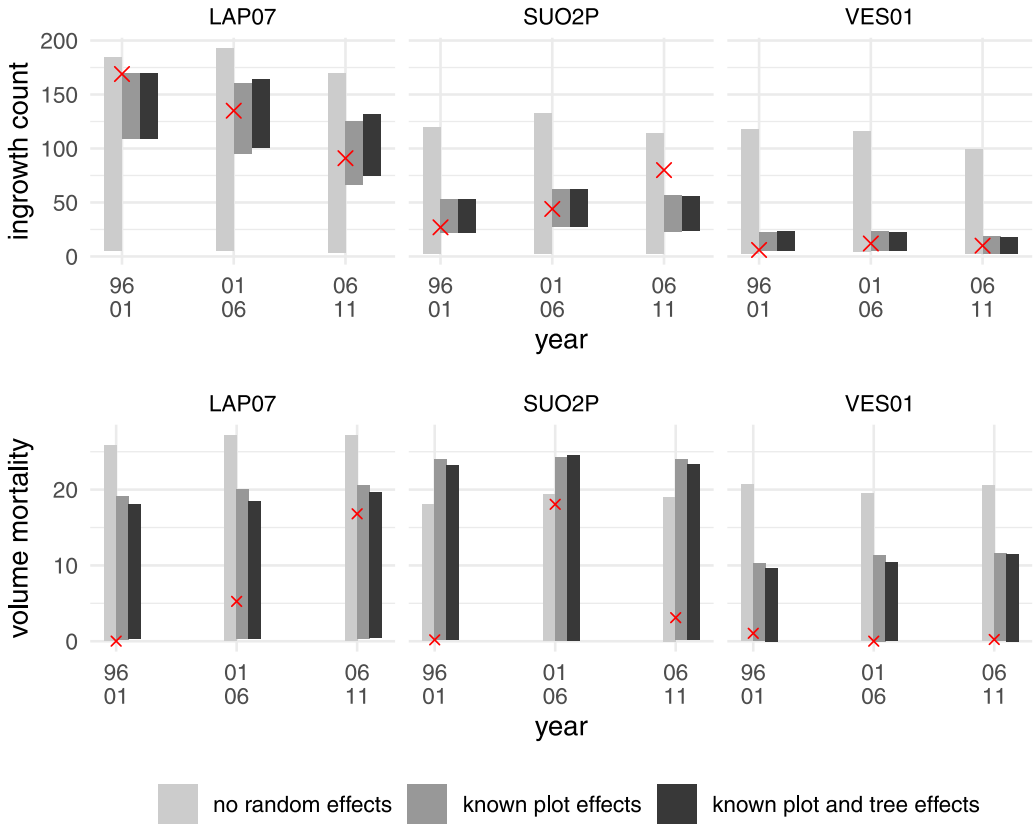

Fig. 6. The number of ingrowth trees and the volume per hectare of the dead trees (mortality, m^3/ha) during the three five-year-periods ending in 2001, 2006 and 2011 for the three plots VES01, LAP07, SUO2P. The red crosses represent the observed values. Different scenarios (see Section 2.3.4) are shown in different gray bars. The area covered by each of the three different gray bars corresponds to the 95% global envelopes computed from the posterior predictive distribution based on 5-year time steps.

trees, particularly since the boreal forest is known to be nutrient-poor and ingrowth trees compete with parent trees (Högberg et al., 2021). From the practical point of view of model application, the incomplete description of the spatial pattern of the smallest trees is a minor issue, because the dispersion of trees with a stem diameter larger than 5 cm was simulated sufficiently well (Fig. 5). Since most of the small trees are removed or die rather early, the modeling of ingrowth trees just needs to coincide with an appropriate density and sufficiently realistic spatial pattern of the remaining trees. Furthermore, the stem diameter and height distributions were also adequately simulated (Fig. 4 and the Figures S3–S5 in the Supplementary Materials). Size distributions such as stem diameter distributions are important in CCF, since they are a crucial characteristic of forest structure and they are also related to demographic and self-organization processes on which CCF heavily relies (Pommerening, 2023).

The tree model could be further extended, e.g., to include separate models for different species, but this may require a more extensive and diverse data set. The dominance of Norway spruce in our data is motivated by the experience that from among the three most common and commercially important tree species (Scots pine, Norway spruce and birch species), only Norway spruce can regenerate and survive when selective cuttings are applied on the fertile sites of Southern Finland (Kellomäki, 2022).

While growth conditions during the growing season may cause quite high variation in the growth and ingrowth rates of a given year (Mäkinen et al., 2022), we included the location-specific time varying temperature sum as an explanatory variable in our ingrowth and growth sub-models. An extension here may include annual random effects, but their derivation from longer observation periods can require more extensive approximations or changes to the current tree model. For example, if an annual random effect is normally distributed, the accumulated random effect on the observation period is not. Thus, such a model no longer fits the brms framework (see Section 2.3.1).

In our long-term simulations, we applied a simple thinning method where trees were thinned in a random fashion without considering their locations; this can be further extended to include more reasonable alternatives that take the current spatial neighborhood of trees into account, as is commonly done in CCF practice. However, the selected approach demonstrates sufficiently well how uncertainty is propagated across years in long-term simulations.

There were also some unexpected factors that affected the growth or death of trees and thus the stand basal area during the period 1996–2011, which were not explicitly included in the model design. As a result of unplanned harvesting or tree mortality caused by forest operations, many trees disappeared between 2001 and 2006 in plot EVO02. This led to an unexpected drop in stand basal area which also affected the spatial characteristics applied in this study, because tree mortality did not occur spatially randomly. There was also a European spruce bark beetle (*Ips typographus* L.) outbreak in Lapinjärvi (LAP) between 2006 and 2011. This is the likely reason for the rather high observed basal area of dead trees in 2011 (Fig. 6), and for the relatively low observed stand basal area in 2011, which is close to the lower bound of the 95% predicted basal area and volume envelopes (Fig. 3). Some storm events occurred in Suonenjoki (SUO) between 2001 and 2006, which caused windthrow and thus decreased the stand basal area in plot SUO2P. As we did not model storm events, our tree model was unable to predict this extraordinarily large basal-area depression.

There are also some issues related to the data that should be noted when interpreting the results. Among the trees that died and were considered as part of tree mortality, wind and snow were the most common causes of mortality. Biotic causes were rare, and some 6% of the total loss in the number of trees could be attributed to inter-tree competition and about 7% to harvesting damage, but for more

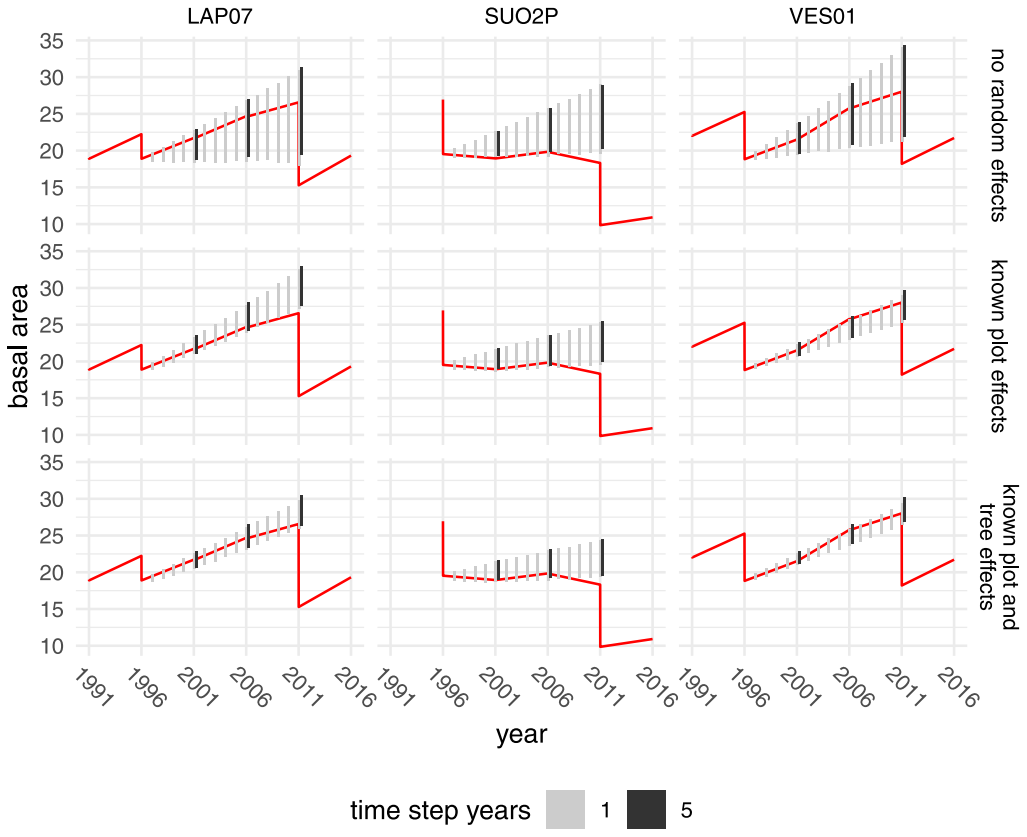

Fig. 7. The total basal area (m^2/ha) of the three plots VES01, LAP07, SUO2P across years when using 1-year and 5-year simulation steps and the three scenarios defined in Section 2.3.4 (rows). Color indicates the step size and the corresponding bars show the 95% global envelopes computed from the posterior predictive distributions.

than half the causes of death remained unknown (Valkonen et al., 2020b). Thus, even though the RBA competition index appeared to explain tree mortality well (Figs. 2), it is not possible to make far-reaching conclusions as to the reasons for why mortality happened. It is interesting that harvesting damage was another important cause of tree mortality (Valkonen et al., 2020b). Particularly when large trees are felled, they may heavily damage neighboring residual trees that eventually die in the aftermath (Pretzsch et al., 2017). With the ongoing introduction of CCF this problem definitely needs to be addressed and forest operators involved in harvesting require more training.

In all our posterior predictive simulations where a random effect was unknown (scenarios (ii) and (iii) in Section 2.3.4), a random effect was drawn from the posterior distribution of a random plot or tree chosen from the data used for modeling. We also tested the alternative that the random effects were instead drawn from the normal distribution that was implied by the posterior distribution of the standard deviation of random effects. The differences between the two alternatives were, however, minor.

We tested various alternatives to different model components. For example, in this study we used the RBA index (Eq. (1)), but we originally tested also other measures of competition, particularly different variants of the Hegyi index (see e.g., Bianchi et al., 2020; Pitkänen et al., 2022) and Gaussian kernels (Pommerening et al., 2011; Häbel et al., 2019). In our exploratory analysis, they showed a performance similar to the selected RBA with very little difference. When selecting measures of competition there are also computational aspects to consider: if measures of competition include parameters to be estimated, these measures must be computed in each iteration of the MCMC. This can be a considerable computational burden. Additionally such a model cannot be specified in the brms package, but Bayesian inference could be implemented for these types of models in Stan (Stan Development Team, 2023). Such an implementation constitutes a considerable amount of additional work and is quite cumbersome in terms of experimenting with the model design. For these reasons, in this study, we settled on the RBA index (Eq. (1)) for explaining growth and mortality, and a corresponding competition field (Eq. (2)) derived from the sum of individual influences of all trees was used in the ingrowth model component.

The simulation results revealed that without knowing the plot and tree random effects, the uncertainties in the simulations can be very high. Furthermore, uncertainty increases rapidly as the simulation period length increases. The poor quality of long-term predictions has been well known (Kangas, 1999; Pretzsch, 2009), but has not yet been properly modeled and included in decision making (de Pellegrin Llorente et al., 2023). The Bayesian approach that we adopted in our tree model might therefore significantly improve the quality of growth simulations especially by producing a realistic description of the uncertainty related to the model parameters. Monte Carlo simulation as used, for example by Kangas (1999), can be applied, too, but taking into account all sources of uncertainty, such as those related to the estimation errors of random effects and non-normality of the parameter estimation errors, can be more easily handled in a Bayesian context. Kangas (1999) also suggested to consider the correlations between the uncertainties of the parameters, which again is straightforward in the Bayesian framework.

In our results, the variation of plot effects led to a variability of stem diameter growth similar to that which is caused by a 11–21 m variability of the site index. Therefore predicting plot effects can potentially give much better information on the growth potential of a site than the traditional site index, which is anyway difficult to estimate correctly in the context of CCF (Pretzsch, 2009). The plot effects can be predicted using measurements of growth of a few sample trees adopting approaches similar to those that have been used, e.g., for predicting tree height–diameter and height–age curves (Mehtätalo and Lappi, 2020;

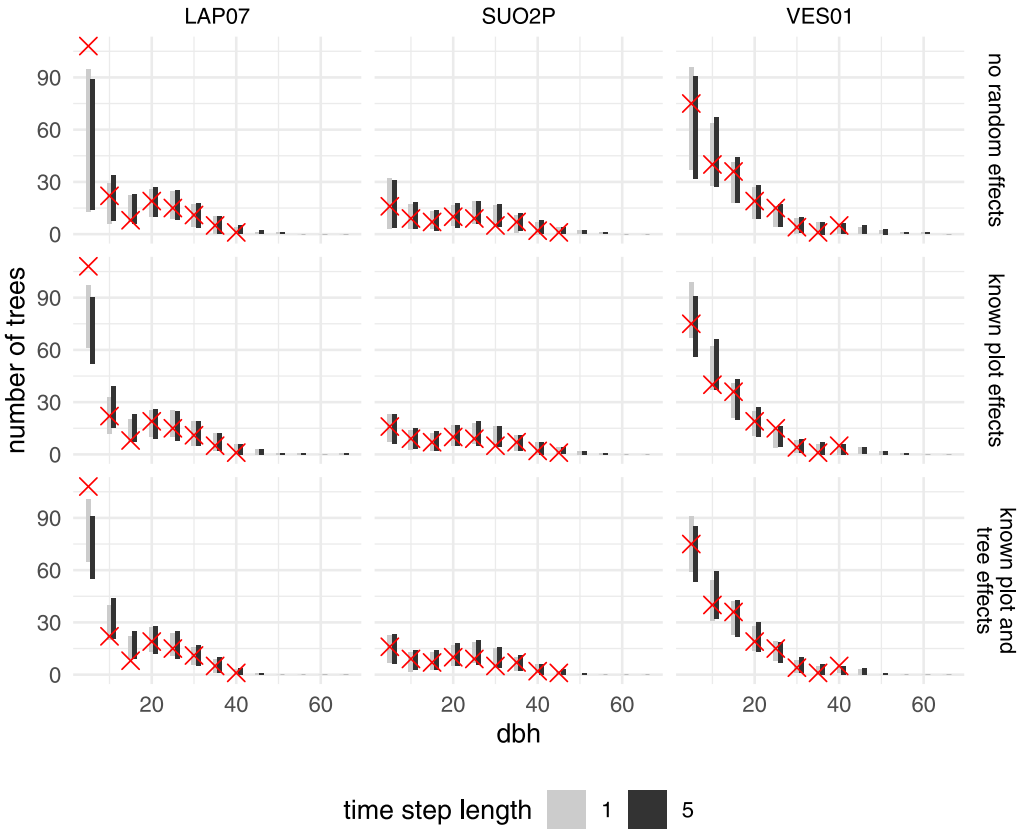

Fig. 8. The numbers of trees in different stem diameter classes in 2011 of the three plots VES01, LAP07, SUO2P when using 1-year and 5-year simulation steps and the three scenarios defined in Section 2.3.4 (rows). Color indicates the step size and the corresponding bars show the 95% global envelopes computed from the posterior predictive distributions.

Sirkiä et al., 2015). The observed strong correlation between the plot effects of stem diameter and height sub-models implies that height measurements, which can be based on LiDAR measurements carried out by drones, could be used to infer information on the plot effects of diameter growth. However, the estimated variability of plot effects was unexpectedly high compared to the effect of the site index, which can have been partially caused by the poor quality and small variability of the site index measurements in our data and by the fact that our plot effects included both variability between plots (within the same stand) and variability between stands. These effects could not be separated because we did not have several plots from the same stand.

5. Conclusions

The simulation results demonstrated that our spatial tree model was sufficiently flexible to adequately describe the dynamics in CCF forests in Southern Finland. Based on the assumption that the observation periods are short in comparison to the corresponding tree growth rates, it turned out to be straightforward to accommodate ingrowth, growth and mortality model components in a generalized multivariate (non)linear multilevel model framework implemented in the R package brms (Bürkner, 2017). This design and the inclusion of spatially explicit competition makes the tree model a versatile alternative to modeling forest dynamics according to various forest management types.

The Bayesian approach allows for straightforward simulations of various quantities from their posterior predictive distributions, thus accounting for uncertainties at different levels and accumulating them over several growth periods (years). We explored these uncertainties in different scenarios. Our experiments suggest that plot or stand effects can have rather high variability; therefore, it makes sense to identify individual-tree growth measurements which can capture this stand effect and to apply it for improved predictions with less uncertainty.

CRediT authorship contribution statement

Mari Myllymäki: Conceptualization, Funding acquisition, Methodology, Writing – original draft, Writing – review & editing. **Mikko Kuronen:** Conceptualization, Formal analysis, Methodology, Visualization, Writing – review & editing. **Simone Bianchi:** Conceptualization, Data curation, Writing – review & editing. **Arne Pommerening:** Conceptualization, Writing – review & editing. **Lauri Mehtätalo:** Conceptualization, Methodology, Writing – review & editing.

Declaration of competing interest

The authors declare that they have no known competing financial interests or personal relationships that could have appeared to influence the work reported in this paper.

Data availability

Data will be made available on request.

Acknowledgments

MM, MK and LM were financially supported by the Research Council of Finland (project numbers 295100, 327211) under Research Council of Finland's flagship ecosystem for Forest-Human–Machine Interplay – Building Resilience, Redefining Value Networks and Enabling Meaningful Experiences (UNITE) (decision numbers 337655, 357909). The authors thank Sauli Valkonen for discussions on the ERIKA data, and Hilkka Ollikainen and Juhani Korhonen for maintaining and measuring the plots of the ERIKA data set. The authors wish to acknowledge CSC – IT Center for Science, Finland, for computational resources.

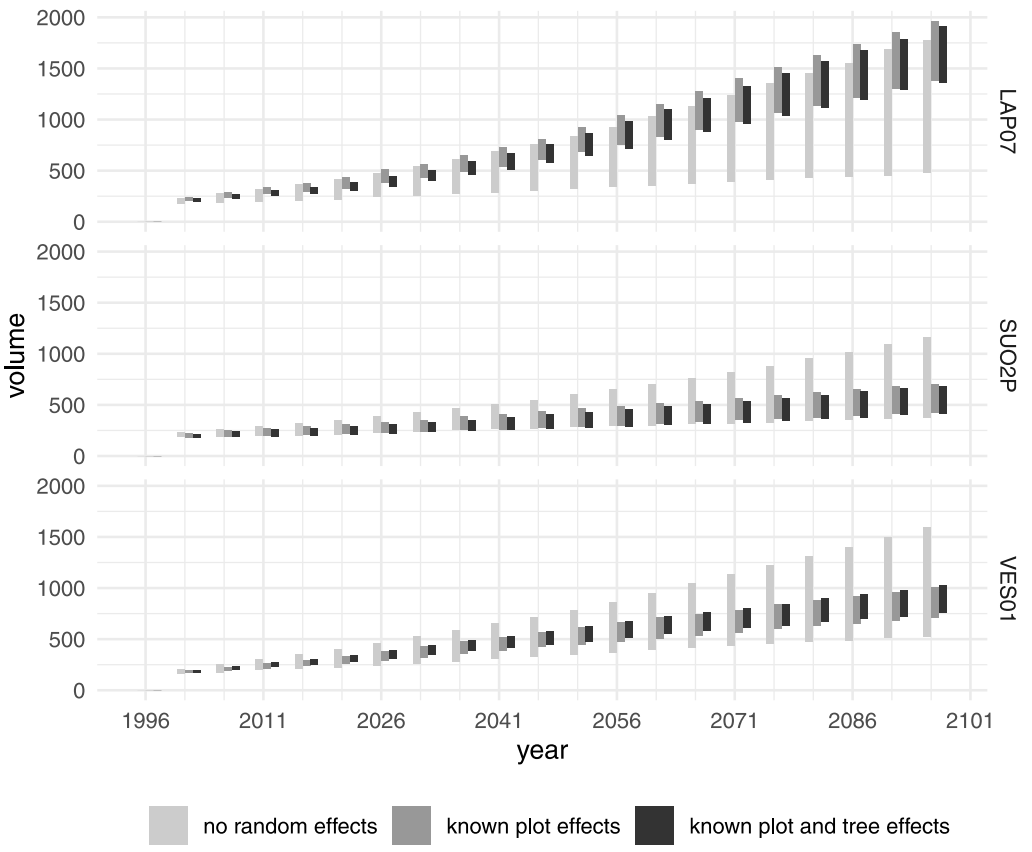

Fig. 9. Total yield (volume m^3/ha) in the three plots LAP07, SUO2P and VES01 across 100 years when using 5-year step simulations and thinning intensity according to official recommendations. The three different scenarios (see Section 2.3.4) are shown in different gray bars. The area covered by each of the three different gray bars corresponds to the 95% global envelopes computed from the posterior predictive distributions.

Appendix A. Supplementary data

Supplementary material related to this article can be found online at https://doi.org/10.1016/j.ecolmodel.2024.110669.

References

Bianchi, S., Myllymäki, M., Siipilehto, J., Salminen, H., Hynynen, J., Valkonen, S., 2020. Comparison of spatially and nonspatially explicit nonlinear mixed effects models for Norway spruce individual tree growth under single-tree selection. Forests 11, http://dx.doi.org/10.3390/f11121338.

Biging, G.S., Dobbertin, M., 1995. Evaluation of competition indices in individual tree growth models. For. Sci. 41, 360–377. http://dx.doi.org/10.1093/forestscience/41.2.360.

Bürkner, P.C., 2017. brms: An R package for Bayesian multilevel models using Stan. J. Stat. Softw. 80, 1–28. http://dx.doi.org/10.18637/jss.v080.i01.

Cajander, A., 1949. Forest types and their significance. Acta For. Fenn. 56, http://dx.doi.org/10.14214/aff.7396.

Cronie, O., Nyström, K., Yu, J., 2013. Spatiotemporal modeling of swedish scots pine stands. For. Sci. 59, 505–516.

Eerikäinen, K., Miina, J., Valkonen, S., 2007. Models for the regeneration establishment and the development of established seedlings in uneven-aged, norway spruce dominated forest stands of southern finland. Forest Ecol. Manag. 242, 444–461. http://dx.doi.org/10.1016/j.foreco.2007.01.078.

Eerikäinen, K., Valkonen, S., Saksa, T., 2014. Ingrowth, survival and height growth of small trees in uneven-aged picea abies stands in southern finland. For. Ecosyst. 1, 5. http://dx.doi.org/10.1186/2197-5620-1-5.

Franklin, J.F., Johnson, K.N., Johnson, D.L., 2018. Ecological Forest Management. Waveland Press Inc., Long Grove.

Garcia, O., 2014. A generic approach to spatial individual-based modelling and simulation of plant communities. Math. Comput. For. Nat.-Resour. Sci. (MCFNS) 6, 36–47, (12).

Gelman, A., Carlin, J.B., Stern, H.S., Dunson, D.B., Vehtari, A., Rubin, D.B., 2014. Bayesian Data Analysis, third ed. Chapman & Hall/CRC, Boca Raton.

Green, E.J., Strawderman, W.E., 1996. A Bayesian growth and yield model for slash pine plantations. J. Appl. Stat. 23, 285–300. http://dx.doi.org/10.1080/02664769624251.

Häbel, H., Myllymäki, M., Pommerening, A., 2019. New insights on the behaviour of alternative types of individual-based tree models for natural forests. Ecol. Model. 406, 23–32. http://dx.doi.org/10.1016/j.ecolmodel.2019.02.013.

Hertog, I.M., Brogaard, S., Krause, T., 2022. Barriers to expanding continuous cover forestry in Sweden for delivering multiple ecosystem services. Ecosyst. Serv. 53, 101392. http://dx.doi.org/10.1016/j.ecoser.2021.101392.

Högberg, P., Wellbrock, N., Högberg, M.N., Mikaelsson, H., Stendahl, J., 2021. Large differences in plant nitrogen supply in German and Swedish forests – Implications for management. Forest Ecol. Manag. 482, 118899. http://dx.doi.org/10.1016/j.foreco.2020.118899.

Hynynen, J., Eerikäinen, K., Mäkinen, H., Valkonen, S., 2019. Growth response to cuttings in norway spruce stands under even-aged and uneven-aged management. Forest Ecol. Manag. 437, 314–323. http://dx.doi.org/10.1016/j.foreco.2018.12.032.

Hynynen, J., Ojansuu, R., Hökkä, H., Siipilehto, J., Salminen, H., Haapala, P. (Eds.), 2002. Models for Predicting Stand Development in MELA System. In: Metsäntutkimuslaitoksen Tiedonantoja, Number 835, Finnish Forest Research Institute, Vantaa Research Centre, Vantaa.

Illian, J., Penttinen, A., Stoyan, H., Stoyan, D., 2008. Statistical Analysis and Modelling of Spatial Point Patterns, first ed. In: Statistics in Practice, John Wiley & Sons, Ltd, Chichester.

Kangas, A.S., 1999. Methods for assessing uncertainty of growth and yield predictions. Can. J. Forest Res. 29, 1357–1364. http://dx.doi.org/10.1139/x99-100.

Kangas, A., Pitkänen, T.P., Mehtätalo, L., Heikkinen, J., 2023. Mixed linear and non-linear tree volume models with regional parameters to main tree species in Finland. Forestry 96, 188–206. http://dx.doi.org/10.1093/forestry/cpac038.

Kellomäki, S., 2022. Management of Boreal Forests: Theories and Applications for Ecosystem Services. Springer International Publishing, Cham, http://dx.doi.org/10.1007/978-3-030-88024-8.

Kruse, L., Erefur, C., Westin, J., Ersson, B.T., Pommerening, A., 2023. Towards a benchmark of national training requirements for continuous cover forestry (CCF) in Sweden. Trees For. People 12, 100391. http://dx.doi.org/10.1016/j.tfp.2023.100391.

Kuronen, M., Särkkä, A., Vihola, M., Myllymäki, M., 2021. Hierarchical log Gaussian Cox process for regeneration in uneven-aged forests. Environ. Ecol. Stat. http://dx.doi.org/10.1007/s10651-021-00514-3.

Kuuluvainen, T., Tahvonen, O., Aakala, T., 2012. Even-aged and uneven-aged forest management in boreal Fennoscandia: A review. AMBIO 41, 720–737. http://dx.doi.org/10.1007/s13280-012-0289-y.

Lappi, J., Bailey, R.L., 1988. A height prediction model with random stand and tree parameters: An alternative to traditional site index methods. For. Sci. 34, 907–927. http://dx.doi.org/10.1093/forestscience/34.4.907.

Lappi, J., Pukkala, T., 2020. Analyzing ingrowth using zero-inflated negative binomial models. Silva Fenn. 54, http://dx.doi.org/10.14214/sf.10370.

Lundqvist, L., 2017. Tamm Review: Selection system reduces long-term volume growth in Fennoscandic uneven-aged Norway spruce forests. Forest Ecol. Manag. 391, 362–375. http://dx.doi.org/10.1016/j.foreco.2017.02.011.

Mäkinen, H., Nöjd, P., Helama, S., 2022. Recent unexpected decline of forest growth in North Finland: examining tree-ring, climatic and reproduction data. Silva Fenn. 56.

Mbogga, M.S., Hamann, A., Wang, T., 2009. Historical and projected climate data for natural resource management in western Canada. Agricult. Forest Meteorol. 149, 881–890. http://dx.doi.org/10.1016/j.agrformet.2008.11.009.

Mehtätalo, L., Lappi, J., 2020. Biometry for Forestry and Environmental Data: With Examples in R. Chapman and Hall/CRC, New York, http://dx.doi.org/10.1201/9780429173462.

Mehtätalo, L., Peltola, H., Kilpeläinen, A., Ikonen, V.P., 2014. The response of basal area growth of Scots pine to thinning: A longitudinal analysis of tree-specific series using a nonlinear mixed-effects model. For. Sci. 60, 636–644. http://dx.doi.org/10.5849/forsci.13-059.

Møller, J., Syversveen, A.R., Waagepetersen, R.P., 1998. Log Gaussian Cox processes. Scand. J. Stat. 25, 451–482. http://dx.doi.org/10.1111/1467-9469.00115.

Monserud, R.A., Sterba, H., 1999. Modeling individual tree mortality for Austrian forest species. Forest Ecol. Manag. 113, 109–123. http://dx.doi.org/10.1016/S0378-1127(98)00419-8.

Myllymäki, M., Mrkvička, T., 2023. GET: Global envelopes in r. http://dx.doi.org/10.1002/sim.9236, arXiv:1911.06583 [stat.ME].

Myllymäki, M., Mrkvička, T., Seijo, H., Grabarnik, P., Hahn, U., 2017. Global envelope tests for spatial processes. J. R. Stat. Soc. Ser. B Stat. Methodol. 79, 381–404. http://dx.doi.org/10.1111/rssb.12172.

Nothdurft, A., 2020. Climate sensitive single tree growth modeling using a hierarchical Bayes approach and integrated nested Laplace approximations (INLA) for a distributed lag model. Forest Ecol. Manag. 478, 118497. http://dx.doi.org/10.1016/j.foreco.2020.118497.

Nyström, K., Ståhl, G., 2001. Forecasting probability distributions of forest yield allowing for a Bayesian approach to management planning. Silva Fenn. 35, http://dx.doi.org/10.14214/sf.595.

O'Hara, K.L., 2014. Multiaged Silviculture. Managing for Complex Forest Stand Structures. Oxford University Press, Oxford.

Palik, B.J., D'Amato, A.W., Franklin, J.F., Johnson, K.N., 2021. Ecological Silviculture. Foundations and Applications. Waveland Press Inc., Long Grove.

de Pellegrin Llorente, I., Eyvindson, K., Mazziotta, A., Lämås, T., Eggers, J., Öhman, K., 2023. Perceptions of uncertainty in forest planning: contrasting forest professionals' perspectives with the latest research. Can. J. Forest Res. 53, 391–406. http://dx.doi.org/10.1139/cjfr-2022-0193, publisher: NRC Research Press.

Peng, C., 2000. Growth and yield models for uneven-aged stands: past, present and future. Forest Ecol. Manag. 132, 259–279. http://dx.doi.org/10.1016/S0378-1127(99)00229-7.

Pitkänen, T., Bianchi, S., Kangas, A., 2022. Quantifying the effects of competition on the dimensions of Scots pine and Norway spruce crowns. Int. J. Appl. Earth Obs. Geoinf. 112, 102941. http://dx.doi.org/10.1016/j.jag.2022.102941.

Pommerening, A., 2023. Continuous Cover Forestry: Theories, Concepts and Implementation. Wiley & Sons Ltd.

Pommerening, A., Gonçalves, A.C., Rodríguez-Soalleiro, R., 2011. Species mingling and diameter differentiation as second-order characteristics. Allg. Forst- Jagdztg. 182, 115–129.

Pommerening, A., Grabarnik, P., 2019. Individual-Based Methods in Forest Ecology and Management. Springer International Publishing, Cham, http://dx.doi.org/10.1007/978-3-030-24528-3.

Pommerening, A., Murphy, S., 2004. A review of the history, definitions and methods of continuous cover forestry with special attention to afforestation and restocking. Forestry 77, 27–44. http://dx.doi.org/10.1093/forestry/77.1.27.

Pretzsch, H., 2009. Forest Dynamics, Growth, and Yield. Springer Berlin Heidelberg, Berlin, Heidelberg, pp. 1–39. http://dx.doi.org/10.1007/978-3-540-88307-4_1.

Pretzsch, H., Forrester, D.I., Bauhus, J. (Eds.), 2017. Mixed-Species Forests. Springer, Berlin, Heidelberg, http://dx.doi.org/10.1007/978-3-662-54553-9.

Puettmann, K.J., Wilson, S.M., Baker, S.C., Donoso, P.J., Drössler, L., Amente, G., Harvey, B.D., Knoke, T., Lu, Y., Nocentini, S., Putz, F.E., Yoshida, T., Bauhus, J., 2015. Silvicultural alternatives to conventional even-aged forest management - what limits global adoption? For. Ecosyst. 2, 8. http://dx.doi.org/10.1186/s40663-015-0031-x.

Pukkala, T., 2018. Instructions for optimal any-aged forestry. Forestry 91, 563–574. http://dx.doi.org/10.1093/forestry/cpy015.

Redenbach, C., Särkkä, A., 2013. Parameter estimation for growth interaction processes using spatio-temporal information. Comput. Statist. Data Anal. 57, 672–683. http://dx.doi.org/10.1016/j.csda.2012.08.006.

Reineke, L.H., 1933. Perfecting a stand-density index for evenaged forests. J. Agric. Res. 46, 627–638.

Rue, H., Martino, S., Chopin, N., 2009. Approximate Bayesian inference for latent Gaussian models using integrated nested Laplace approximations (with discussion). J. R. Stat. Soc. Ser. B Stat. Methodol. 71, 319–392.

Salas-Eljatib, C., 2020. Height growth–rate at a given height: A mathematical perspective for forest productivity. Ecol. Model. 431, 109198. http://dx.doi.org/10.1016/j.ecolmodel.2020.109198.

Schneider, M.K., Law, R., Illian, J.B., 2006. Quantification of neighbourhood-dependent plant growth by Bayesian hierarchical modelling. J. Ecol. 94, 310–321. http://dx.doi.org/10.1111/j.1365-2745.2005.01079.x.

Siipilehto, J., Sarkkola, S., Nuutinen, Y., Mehtätalo, L., 2023. Predicting height-diameter relationship in uneven-aged stands in Finland. Forest Ecol. Manag. 549, 121486. http://dx.doi.org/10.1016/j.foreco.2023.121486.

Sirkiä, S., Heinonen, J., Miina, J., Eerikäinen, K., 2015. Subject-specific prediction using a nonlinear mixed model: Consequences of different approaches. For. Sci. 61, 205–212. http://dx.doi.org/10.5849/forsci.13-142.

Skovsgaard, J.P., Vanclay, J.K., 2008. Forest site productivity: a review of the evolution of dendrometric concepts for even-aged stands. Forestry 81, 13–31. http://dx.doi.org/10.1093/forestry/cpm041.

Stan Development Team, 2022. Stan modeling language users guide and reference manual, 2.30. https://mc-stan.org.

Stan Development Team, 2023. RStan: the R interface to Stan. URL: https://mc-stan.org/. [r package version 2.21.8].

Tapio, 2023. Best practices for sustainable forest management. https://metsanhoidonsuositukset.fi/en. Accessed: 2023-06-05.

Tonteri, T., Hotanen, J.P., Kuusipalo, J., 1990. The Finnish forest site type approach: ordination and classification studies of mesic forest sites in southern finland. Vegetatio 87, 85–98. http://dx.doi.org/10.1007/bf00045658.

Valkonen, S., Aulus Giacosa, L., Heikkinen, J., 2020a. Tree mortality in the dynamics and management of uneven-aged Norway spruce stands in southern Finland. Eur. J. For. Res. 139, 989–998. http://dx.doi.org/10.1007/s10342-020-01301-8.

Valkonen, S., Giacosa, L.A., Heikkinen, J., 2020b. Tree mortality in the dynamics and management of uneven-aged norway spruce stands in southern finland. Eur. J. For. Res. 139, 989–998. http://dx.doi.org/10.1007/s10342-020-01301-8.

Wilson, D., Monleon, V., Weiskittel, A., 2019. Quantification and incorporation of uncertainty in forest growth and yield projections using a Bayesian probabilistic framework: A demonstration for plantation coastal Douglas-fir in the Pacific Northwest, USA. Math. Comput. For. Nat.-Resour. Sci. 11, 264–285.

Wyckoff, P.H., Clark, J.S., 2000. Predicting tree mortality from diameter growth: a comparison of maximum likelihood and Bayesian approaches. Can. J. Forest Res. 30, 156–167. http://dx.doi.org/10.1139/x99-198, publisher: NRC Research Press.

Wykoff, W.R., 1990. A basal area increment model for individual conifers in the Northern Rocky Mountains. For. Sci. 36, 1077–1104. http://dx.doi.org/10.1093/forestscience/36.4.1077.

Zhou, M., Lei, X., Lu, J., Gao, W., Zhang, H., 2022. Comparisons of competitor selection approaches for spatially explicit competition indices of natural spruce-fir-broadleaf mixed forests. Eur. J. For. Res. 141, 177–211. http://dx.doi.org/10.1007/s10342-021-01430-8.